Supplement of Atmos. Chem. Phys., 25, 16063–16083, 2025 https://doi.org/10.5194/acp-25-16063-2025-supplement © Author(s) 2025. CC BY 4.0 License.





Supplement of

Aircraft in-situ measurements from SOCRATES constrain the anthropogenic perturbations of cloud droplet number

Ci Song et al.

Correspondence to: Ci Song (csong@uwyo.edu)

The copyright of individual parts of the supplement might differ from the article licence.

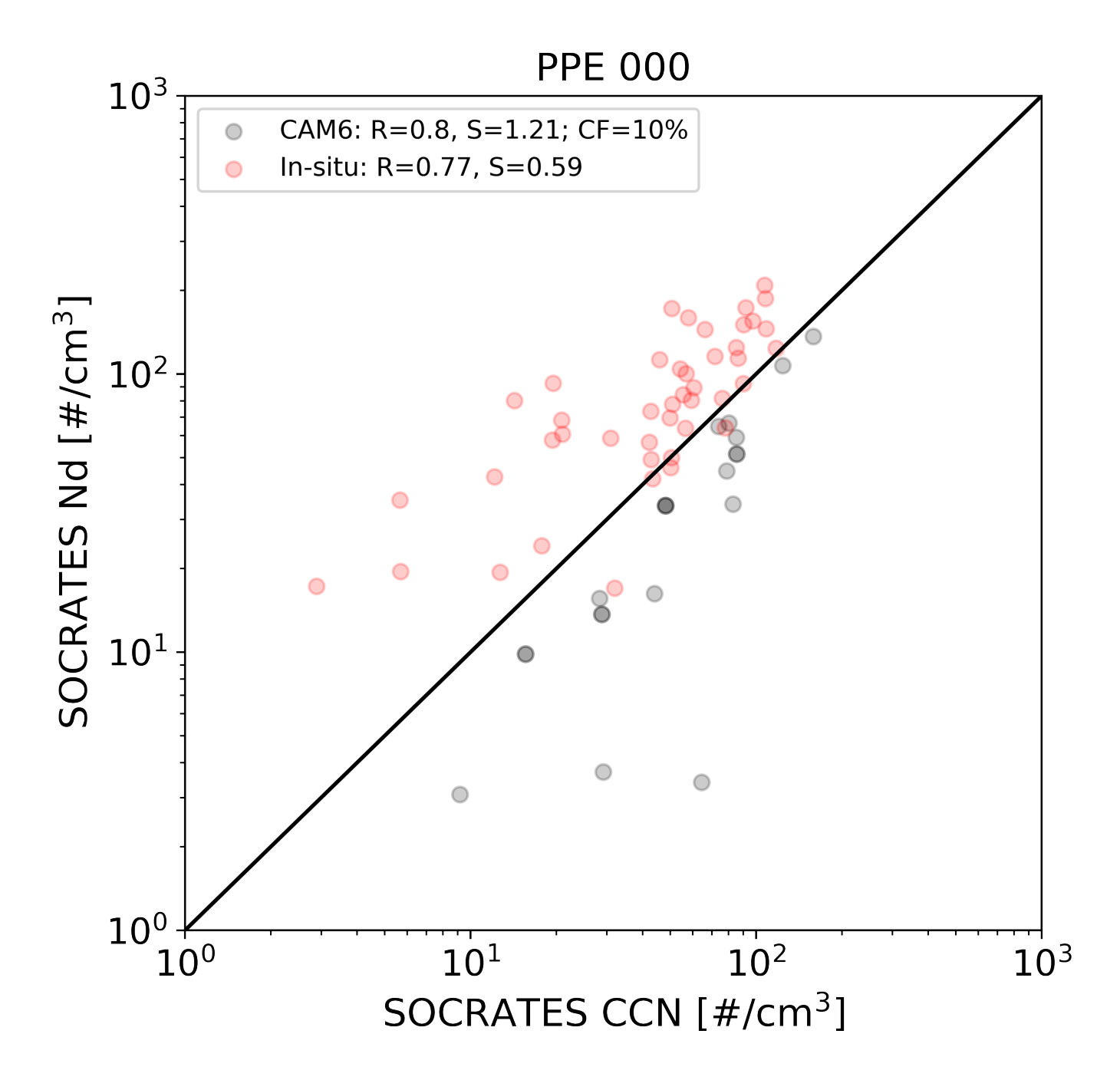


Figure S1: Relationship between SOCRATES CCN and cloud droplet number concentration (Nd) from flight composites from CAM6 default configuration (black dots) and in-situ measurements (red dots). Model outputs are collocated with in-situ measurements from flight tracks by 50 m x 2 min bin means. Same with Figure 2 in the main text but using a threshold of liquid cloud fraction $\geq 10\%$ for in-cloud N_d .

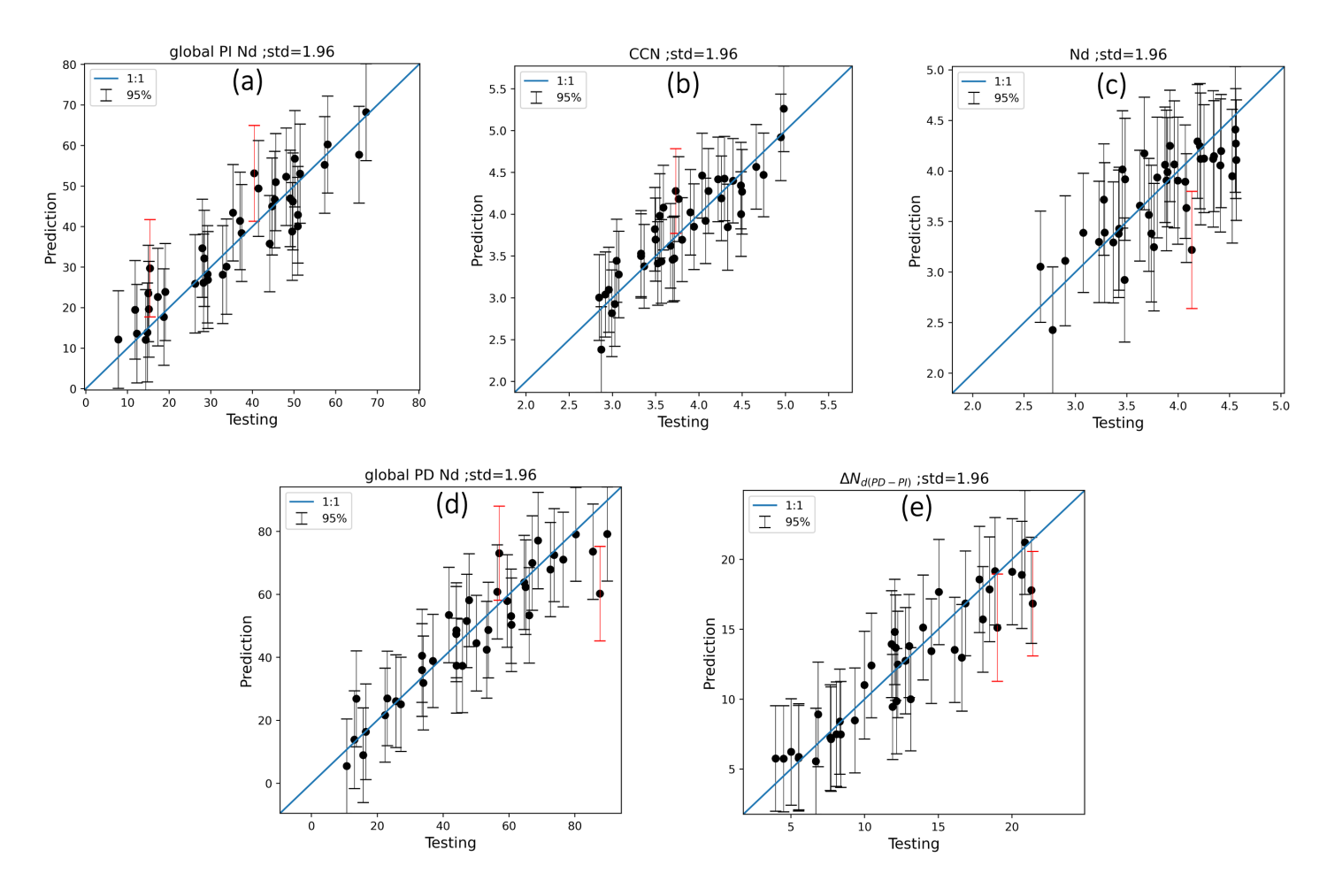


Figure S2: Emulator predictions for each emulator used in this study. For each model output (a-e), the value for the model output for the 40 validation runs is plotted against the mean predictions by the emulator (black dots). The vertical lines are 95% bounds of emulator uncertainty on the emulator mean predictions. Emulator uncertainties overlapped with validation runs are shown in black vertical lines. Otherwise in red.

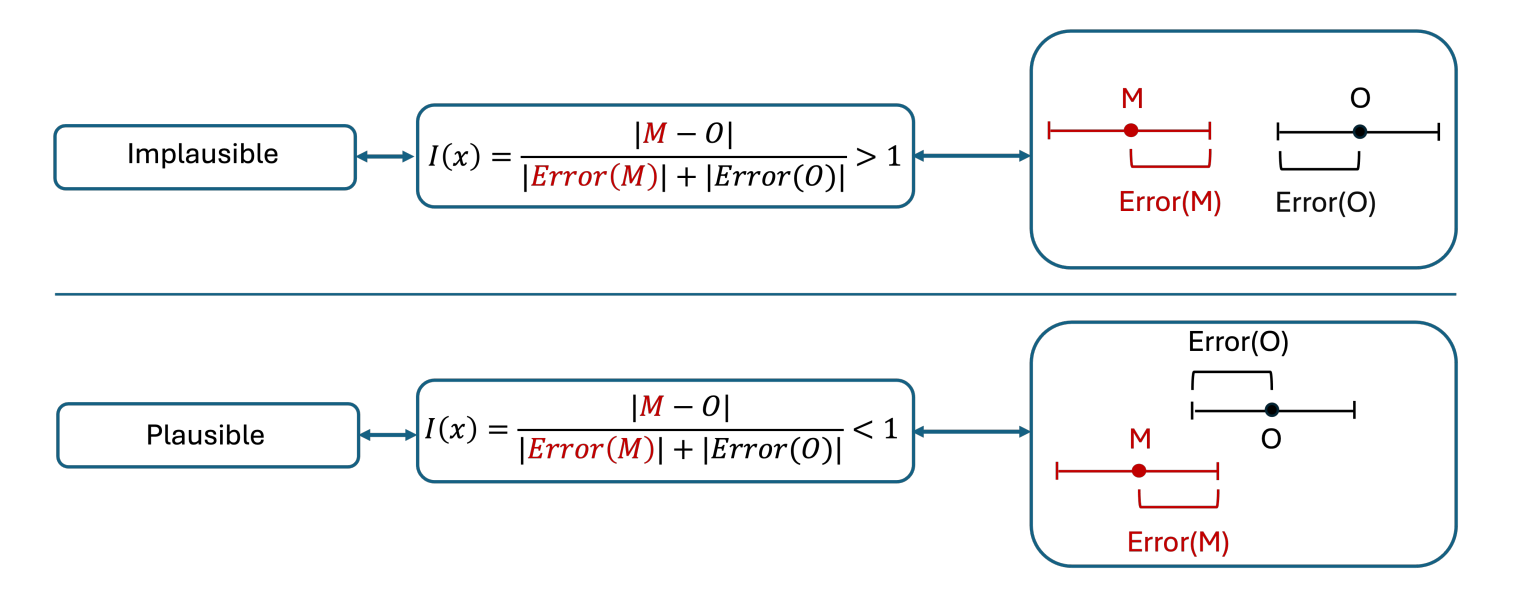


Figure S3: An illustration of our constraint process in Eq 1. M is the emulator campaign mean and O is the observationally-campaign mean. Error(M) and Error(O) denotes the deviation from the emulator campaign mean and observation campaign mean, respectively. Error(M) comes from emulator uncertainty and can be directly calculated from GP regression. Observation uncertainty is from instrument errors, sampling strategies and environmental noises. Briefly, models variants are excluded as implausible when the distance between emulator mean and observation mean is greater than the sum of their uncertainties $((|M| + |O|) \ge (|Error(M)| + |Error(O)|)$.

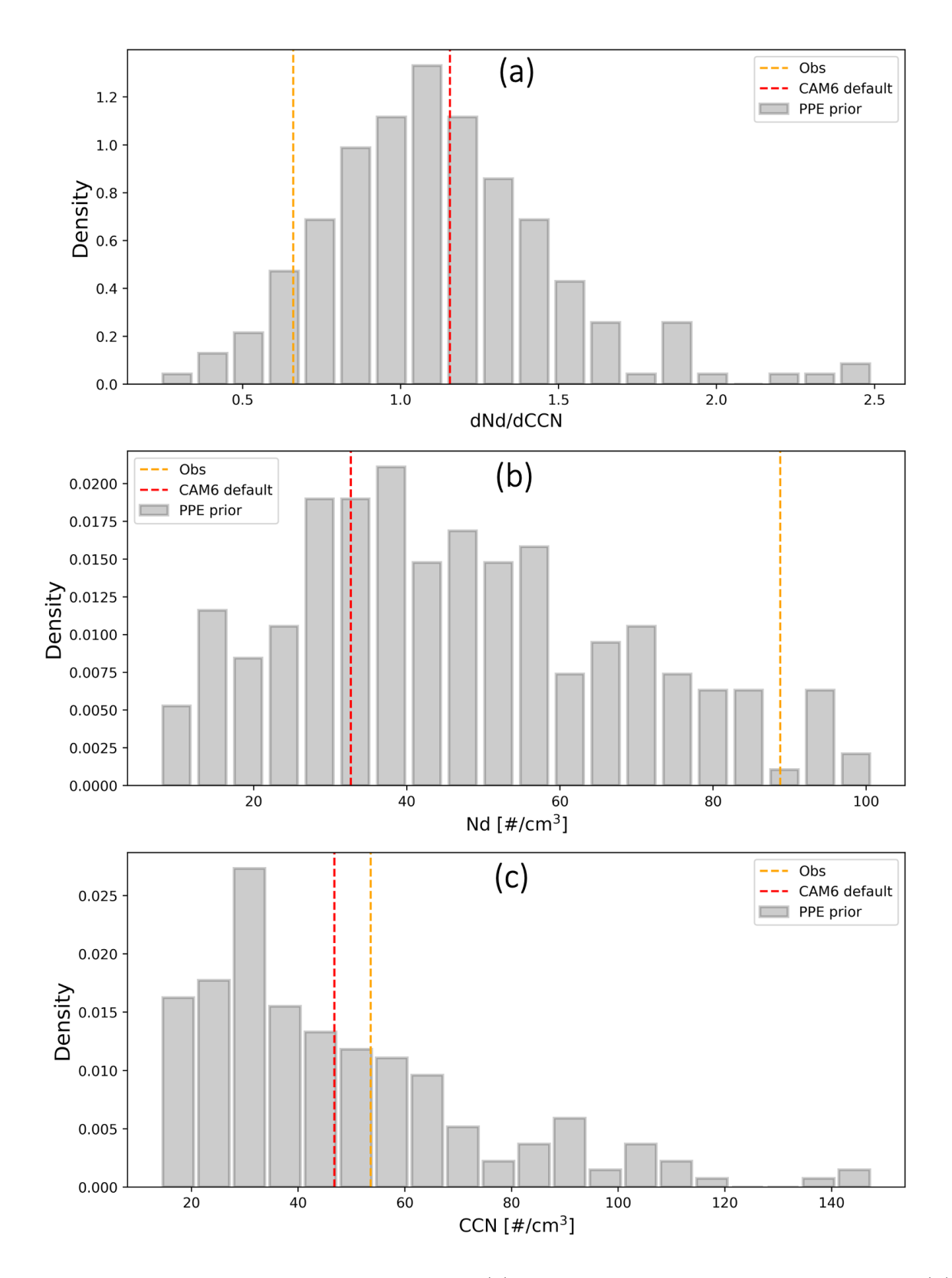


Figure S4: Probability distributions of the (a) linear regression slope of N_d on CCN, (b) N_d and (c) CCN from the CAM6 PPE flight composites (50 m x 2 min bin means, matched by space and time) collocated to in-situ flight track measurements (orange). CAM6 default is shown in red dashed lines.

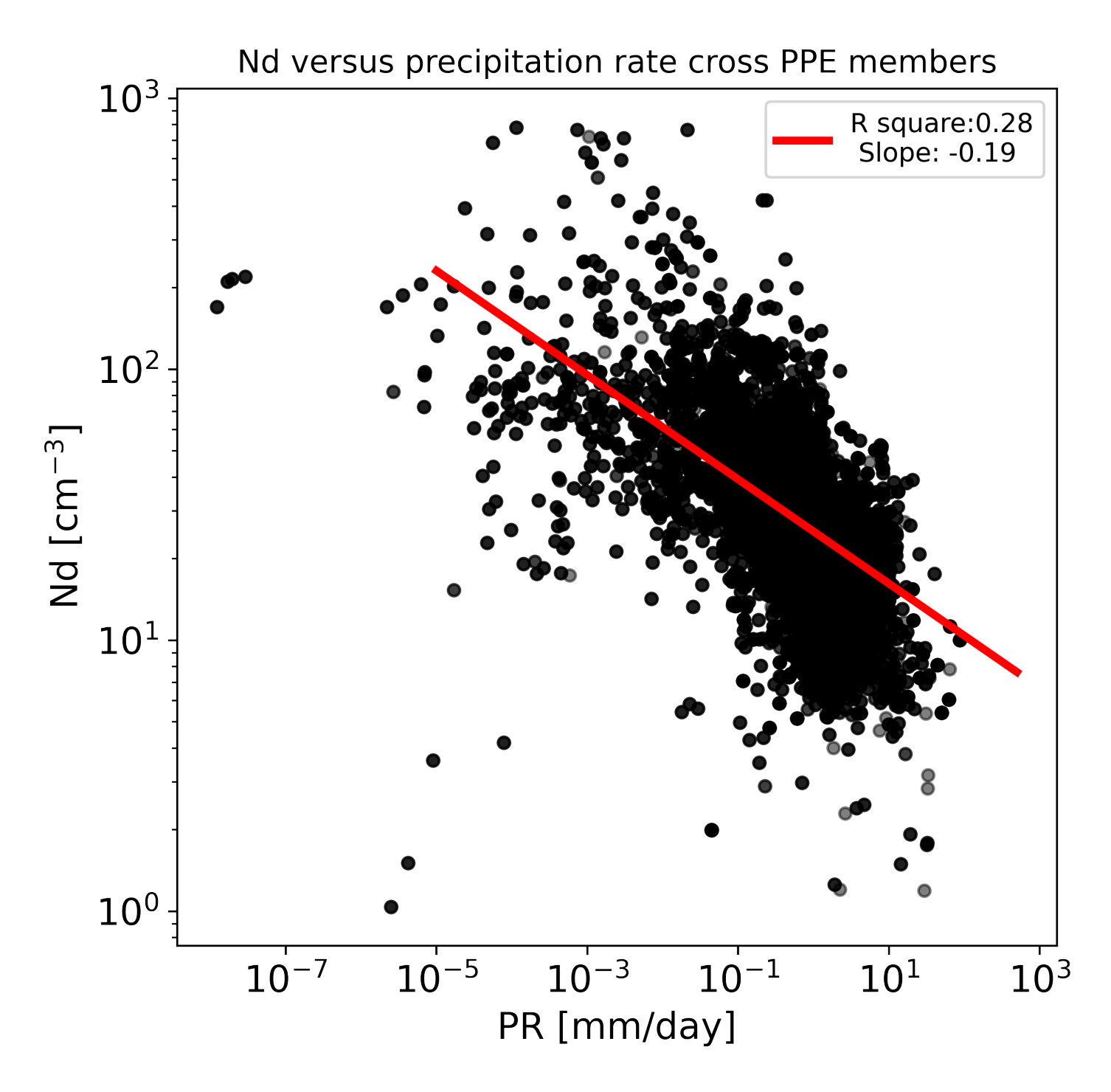


Figure S5: Nd versus precipitation rate. Each dot represents one simulation time step averaged across ensemble members.

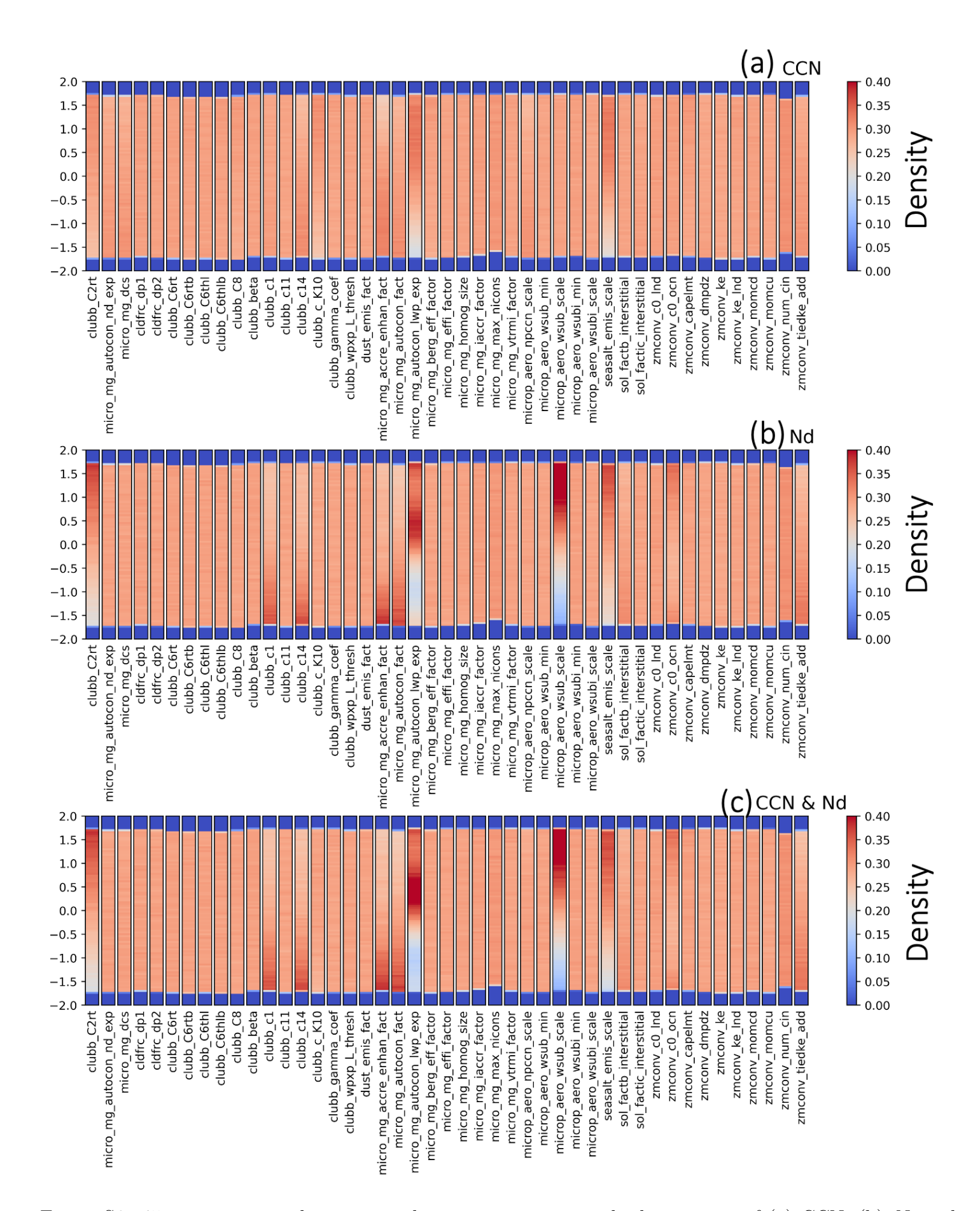


Figure S6: 45 parameters with constrained parameter spaces with observations of (a) CCN, (b) N_d and (c) CCN & N_d . Parameter spaces are standardized with mean 0 and variance 1. Warmer colors mean a higher intensity and more data points in that range.

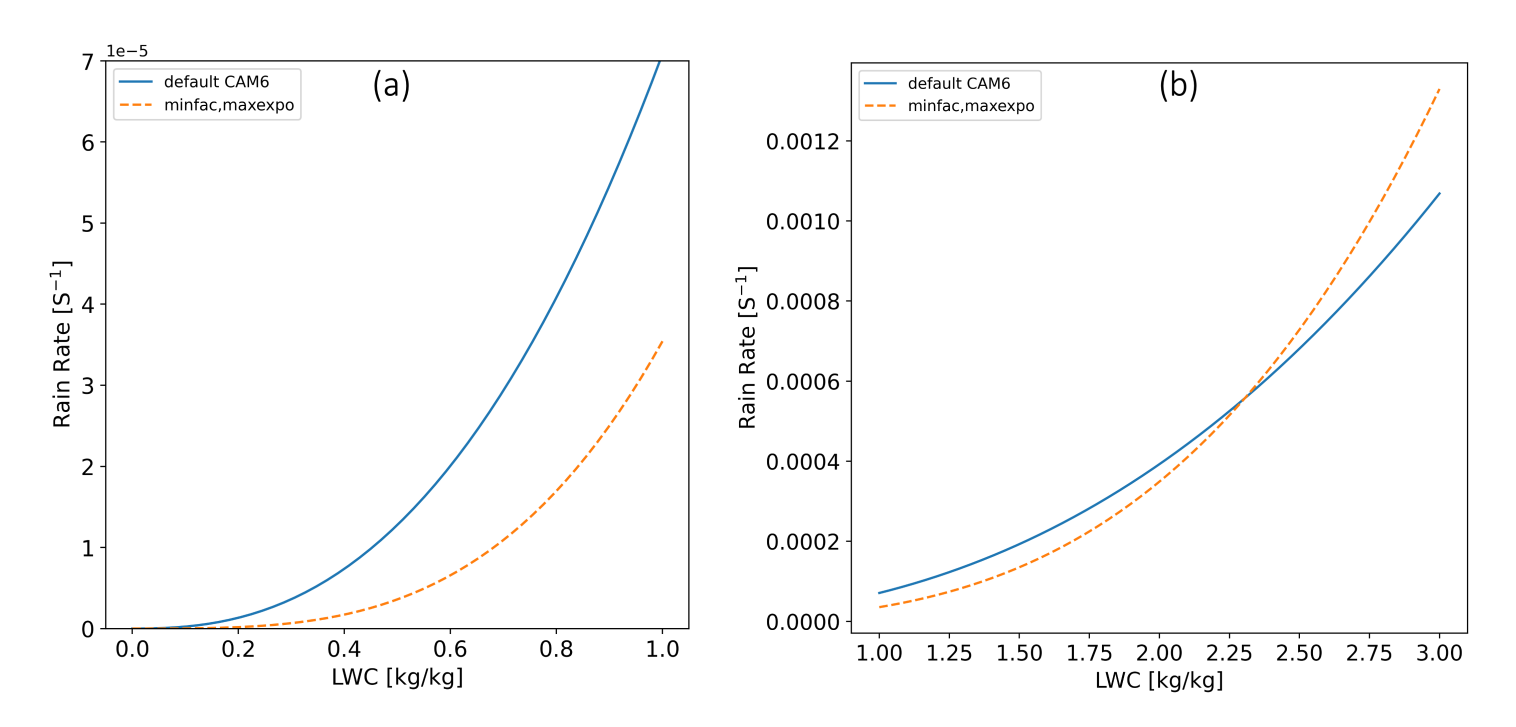


Figure S7: Rain rate [PR: S^{-1}] versus liquid water content [LWC: kg/kg] from CAM6 default configuration (blue) and configuration suggested by observations of CCN from SOCRATES (orange) for which scale factor (a in Eq 7) is minimized and the exponent (b in Eq 7) is maximized. (a) LWC varies between 0 to 1 kg/kg, which is a typical range simulated in CAM6 PPE. Within this LWC range, CAM6 default model overestimates rain rate. (b) LWC varies between 1 to 3 kg/kg. LWC in this range is not possible in CAM6 PPE but we are showing the extreme case at which CAM6 default model might underestimate rain rate at LWC > 2.4 kg/kg.

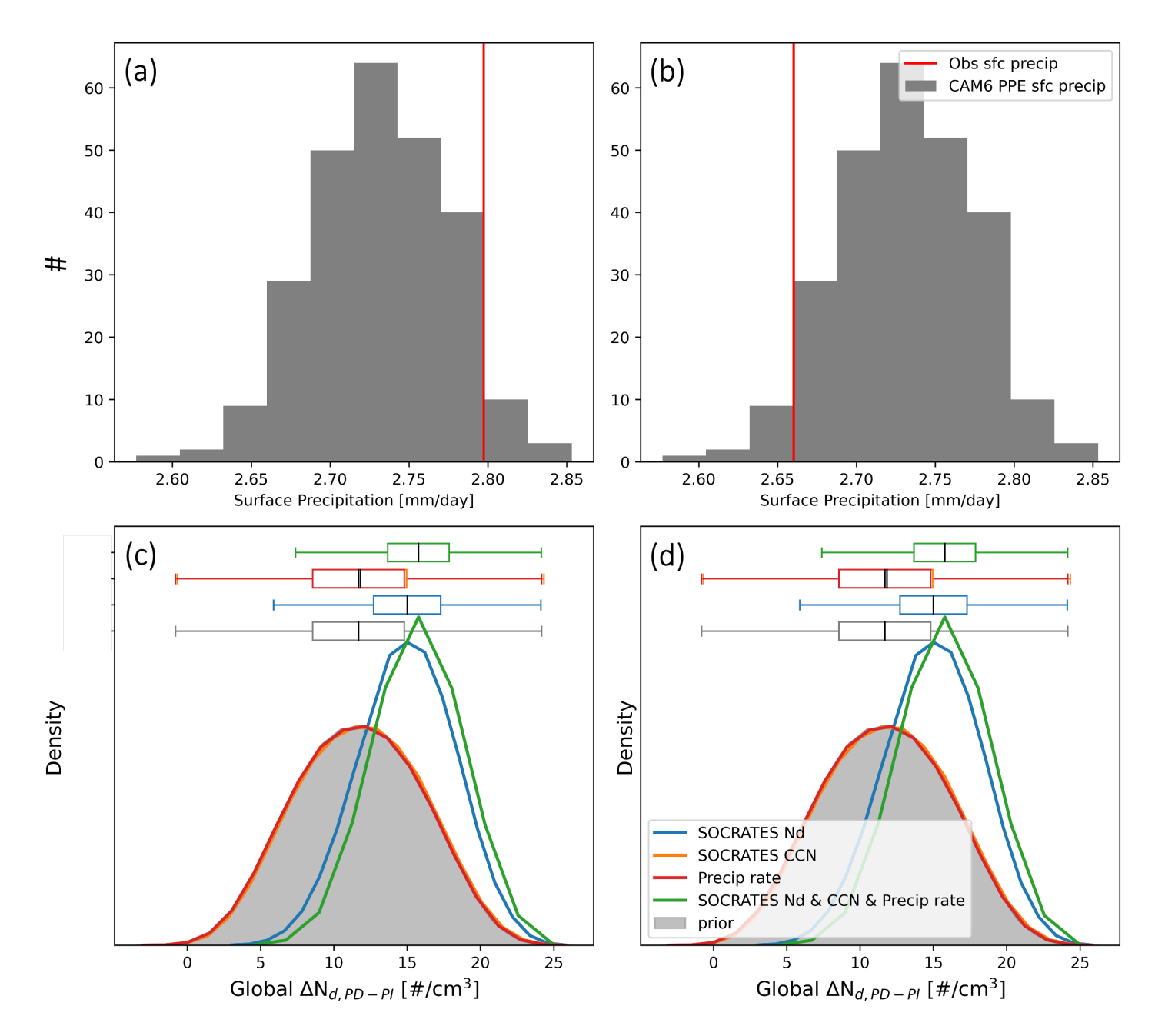


Figure S8: Theoretical scenarios of the distribution of $\Delta N_{d,PD-PI}$ constrained by observations of CCN and N_d , and two hypothetical campaign-mean surface precipitation rates (ac and bd). (a) The distribution of campaign-mean surface precipitation from the CAM6 PPE is shown as histograms. A constraint is applied using a hypothetical campaign-mean surface precipitation rate corresponding to the 95th percentile of the CAM6 PPE distribution, with 20% uncertainty from the mean. The observationally-constrained posterior from SOCRATES observed CCN only (orange), N_d only (blue), hypothetical surface precipitation rate only (red), and combining CCN, N_d and surface precipitation rate (green) is shown in (c). (b) the same with (a) but the CAM6 PPE is constrained by campaign-mean surface precipitation rates corresponds to 5th percentile of the CAM6 PPE distribution, with 20% uncertainty from the mean. (d) the same with (c) but use hypothetical precipitation rate in (b).

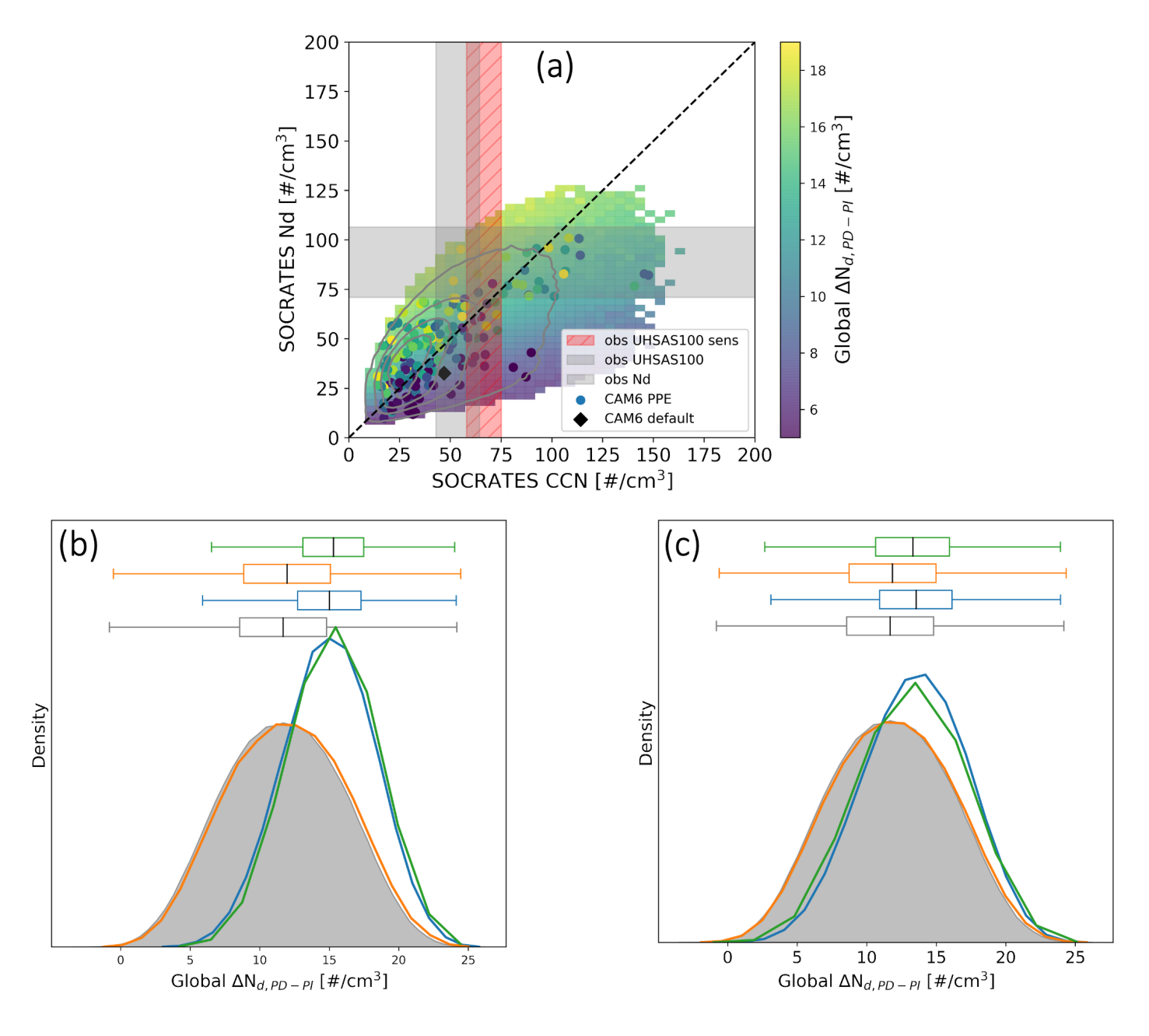


Figure S9: Sensitivity tests on the constraints on $\Delta N_{d,PD-PI}$. (a) Same as Figure 7b, but with CCN increased by 8% and 40% (red shaded bar) relative to the original campaign-mean CCN (gray shaded bar). The 8% and 40% increases represent the lower and upper bounds of CCN uncertainty in our sensitivity tests, respectively. The lower bound is based on the median of the CCN0.2:UHSAS100 ratio, and the upper bound corresponds to the 75th percentile of the CCN0.2:UHSAS100 ratio uncertainty, as reported in McCoy et al. (2021). (b) Similar to Figure 8a but showing the distribution of $\Delta N_{d,PD-PI}$ constrained by observations of CCN and N_d , with CCN increased as described, and emulator uncertainty excluded. (c) Same as (b), but including emulator uncertainty.

Table S1: A description of the parameters that are perturbed and their ranges.

Physics Scheme	Parameter Name	Description	Default	Min	Max	Units
CLUBB	clubb_C2rt	Damping on scalar variances	1.0	0.2	2	-
	clubb_C6rt	Low skewness in C6rt skewness function	4.0	2.0	6	-
	$clubb_C6rtb$	High skewness in C6rt skewness function	6.0	2.0	8	-
	clubb_C6thl	Low skewness in C6thl skewness function	4.0	2.0	6	-
	clubb_C6thlb	High skewness in C6thl skewness function	6.0	2.0	8	-
	clubb_C8	Coef. #1 in C8 skewness Equation	4.2	1.0	5	-
	clubb_beta	Set plume widths for theta_l and rt	2.4	1.6	2.5	-
	clubb_c1	Low Skewness in C1 Skw.	1.0	0.4	3	-
	clubb_c11	Low Skewness in C11 Skw	0.7	0.2	0.8	-
	clubb_c14	Constant for $u^{\prime 2}$ and $v^{\prime 2}$ terms	2.2	0.4	3	-
	clubb_c_K10	Momentum coefficient of Kh_zm	0.5	0.2	1.2	-
	clubb_gamma_coef	Low Skw.: gamma coef. Skw	0.308	0.25	0.35	-
	$clubb_wpxp_L_thresh$	Lscale threshold, damp C6 and C7	60	20	200	m
MG2	micro_mg_accre_enhan_fact	Accretion enhancing factor	1.0	0.1	10.0	-
	micro_mg_autocon_fact	Autoconversion factor	0.01	0.005	0.2	-
	micro_mg_autocon_lwp_exp	KK2000 LWP exponent	2.47	2.10	3.30	-
	micro_mg_autocon_nd_exp	KK2000 autoconversion exponent	-1.1	-0.8	-2	-
	micro_mg_berg_eff_factor	Bergeron efficiency factor	1.0	0.1	1.0	-
	micro_mg_dcs	Autoconversion size threshold ice-snow	500e-06	50e-06	1000e-06	m
	micro_mg_effi_factor	Scale effective radius for optics calculation	1.0	0.1	2.0	-
	micro_mg_homog_size	Homogeneous freezing ice particle size	25e-6	10e-6	200e-6	m
	micro_mg_iaccr_factor	Scaling ice/snow accretion	1.0	0.2	1.0	_
	micro_mg_max_nicons	Maximum allowed ice number concentration	100e6	1e5	10000e6	$\# kg^{-1}$
	micro_mg_vtrmi_factor	Ice fall speed scaling	1.0	0.2	5.0	${ m m~s^{-1}}$
Aerosol	microp_aero_npccn_scale	Scale activated liquid number	1	0.33	3	_
	microp_aero_wsub_min	Min subgrid velocity for liq activation	0.2	0	0.5	${ m m~s^{-1}}$
	microp_aero_wsub_scale	Subgrid velocity for liquid activation scaling	1	0.1	5	-
	microp_aero_wsubi_min	Min subgrid velocity for ice activation	0.001	0	0.2	${ m m~s^{-1}}$
	microp_aero_wsubi_scale	Subgrid velocity for ice activation scaling	1	0.1	5	-
	dust_emis_fact	Dust emission scaling factor	0.7	0.1	1.0	-
	seasalt_emis_scale	Seasalt emission scaling factor	1.0	0.5	2.5	_
	sol_factb_interstitial	Below cloud scavenging of interstitial modal aerosols	0.1	0.1	1	_
	sol_factic_interstitial	In-cloud scavenging of interstitial modal aerosols	0.4	0.1	1	_
ZM	cldfrc_dp1	Parameter for deep convection cloud fraction	0.1	0.05	0.25	_
	cldfrc_dp2	Parameter for deep convection cloud fraction	500	100	1000	-
	zmconv_c0_lnd	Convective autoconversion over land	0.0075	0.002	0.1	m^{-1}
	zmconv_c0_ocn	Convective autoconversion over ocean	0.03	0.02	0.1	m^{-1}
	zmconv_capelmt	Triggering threshold for ZM convection	70	35	350	$ m J~kg^{-1}$
	zmconv_dmpdz	Entrainment parameter	-1.0e-3	-2.0e-3	-2.0e-4	m^{-1}
	zmconv_ke	Convective evaporation efficiency	5.0e-6	1.0e-6	1.0e-5	$(\text{kg m}^{-2} \text{ s}^{-1})^{0.5} \text{ s}^{-1}$
	zmconv_ke_lnd	Convective evaporation efficiency over land	1.0e-5	1.0e-6	1.0e-5	$(\text{kg m}^{-2} \text{ s}^{-1})^{0.5} \text{ s}^{-1}$
	zmconv_momcd	Efficiency of pressure term in ZM downdraft CMT	0.7	0	1.00-5	-
	mconv_momcu	Efficiency of pressure term in ZM updraft CMT	0.7	0	1	_
	ouv -momeu					_
	zmconv_num_cin	Allowed number of negative buoyancy crossings	1	1	5	_